HAL
archives-ouvertes.fr

Self-lubricating polymer composites : using numerical trbology to hightlight their design criterion

Maria Villavicencio, Mathieu Renouf, Aurélien Saulot, Y Michel, Yves Mahéo, Guillaume Colas, Tobin Filleter, Yves Berthier

▶ **To cite this version:**

Maria Villavicencio, Mathieu Renouf, Aurélien Saulot, Y Michel, Yves Mahéo, et al.. Self-lubricating polymer composites : using numerical trbology to hightlight their design criterion . ESMATS 2017, Sep 2017, Hatefiled, United Kingdom. hal-01768786

HAL Id: hal-01768786
https://hal.archives-ouvertes.fr/hal-01768786

Submitted on 17 Apr 2018

HAL is a multi-disciplinary open access archive for the deposit and dissemination of scientific research documents, whether they are published or not. The documents may come from teaching and research institutions in France or abroad, or from public or private research centers.

L'archive ouverte pluridisciplinaire **HAL**, est destinée au dépôt et à la diffusion de documents scientifiques de niveau recherche, publiés ou non, émanant des établissements d'enseignement et de recherche français ou étrangers, des laboratoires publics ou privés.

SELF-LUBRICATING POLYMER COMPOSITES: USING NUMERICAL TRIBOLOGY TO HIGHTLIGHT THEIR DESIGN CRITERION

Villavicencio M. D. [1,2,3,4], Renouf M. [2,6], Saulot A. [1,6], Michel Y. [3], Mahéo Y. [4], Colas G. [5], Filleter T. [5], Berthier Y. [5,6]

[1] *LaMCoS, Université de Lyon, INSA-Lyon, CNRS, Villeurbanne, France. Email: maria.villavicenciorojas@insa-lyon.fr, aurelien.saulot@insa-lyon.fr, yves.berthier@insa-lyon.fr*
[2] *LMGC, Univ. Montpellier, CNRS, Montpellier, France.* Email: mathieu.renouf@umontpellier.fr
[3] *CNES, 18 avenue Edouard Belin, 31401 Toulouse Cedex 9, France. Email: yann.michel@cnes.fr*
[4] SKF Aerospace, F-26300 Châteauneuf-sur-Isère, France. *Email: yves.maheo@skf.com*
[5] *Department of Mechanical and Industrial Engineering, University of Toronto, Toronto, Canada. Email: guillaume.colas@utoronto.ca, filleter@mie.utoronto.ca*
[6] *InTriG, International Tribology Group, Villeurbanne, France.*

ABSTRACT

After the cessation of RT/Duroid 5813, manufacturing tests were performed by CNES and ESA/ESTL in order to find an alternative material. Although PGM-HT was selected as the best candidate, limitations about its tribological capabilities to replace RT/Duroid 5813 were later pointed out. Today, the predictability of the tribological behaviour of those materials is not fully overcome. The motivation to this work is to complement studies of self-lubricating materials by coupling experimental analyses with numerical modelling, in order to predict their tribological behaviour. A Discrete Element Method is chosen to construct the numerical material, because it allows to represent wear and the third body generation at the scale of the ball/retainer contact. An underlying role of the adhesion between components in controlling the tribological properties of the transfer film has been observed.

INTRODUCTION

The accomplishment of spacecraft missions strongly depends on the reliability of mechanisms. This reliability in turn, depends on the life and functionality of their components parts: here lays the importance of space tribology. A recent example is the *Juno mission* to Jupiter, which has been stuck in making long laps around the planet because of "sticky valves" [1].

In space applications, design of the components and of the lubricants must be robust not only to endure the conditions of space, but also the rigours of the launch environment. Both liquid and solid lubricants can be used for space applications. Where temperature and contamination issues exclude the use of fluid lubricants, solid lubrication is used [2]. Self-lubricating composite materials are an example of dry lubricants. They are usually used as the retainer material of ball bearings. The composite is involved in forming a composite transfer film from the cage to both balls and races by intermittent sliding contact at balls/cage contact all along lifetime, so the retainer material itself provides lubrication to the bearing by a mechanism known as double transfer (see Fig.1) [3][4][5]. Among those materials RT/Duroid 5813 and PGM-HT are known for their use in space applications. After the cessation of RT/Duroid 5813 manufacturing, PGM-HT was selected as the best replacement option [6]. Nevertheless, after tribological expertise on lifetests carried out by Sicre et al [3], it was concluded that the performance of PGM-HT as a replacement for Duroid should be improved. For PGM-HT as for RT/Duroid 5813 its composition remain still not fully known, despite the fact that the importance of the composite microstructure on the tribological performances has been previously pointed out [3][4][7][8], the role and impact of the different constituents on the degradation and lubrication mechanisms remain not well understood (as the size of the fillers, the microstructure, or the volume fraction).

In this work, it is proposed to couple an experimental and a numerical approach in order to complement the on-going studies that investigate self-lubricating materials with a focus on PGM-HT composite. An accurate simulation of the double transfer mechanism is not an easy task: the whole mechanism should be represented (for example the bearing and its solicitations), the degradation of the composite material and the evolution of the debris within the system. Despite modelling the whole system is desired, it is possible to have a local approach to identify the possible scenarios of double transfer mechanisms. For such a model, Discrete Element framework appears as the most appropriate tools to describe third body flows [9] (from material degradation to wear). An equivalent numerical approach has already been used in the context of C/C composites [10]. In the present work, the approach is extended to self-lubricating composites. As a first approach a single contact is taken into account, and only an elementary volume of the cage/ball contact is considered. A meshless strategy is used, and the volume is discretized with circular rigid bodies. Consisting of independent elements, a discrete element modelling must integrate interaction laws between the elements to enable to describe both the overall mechanical

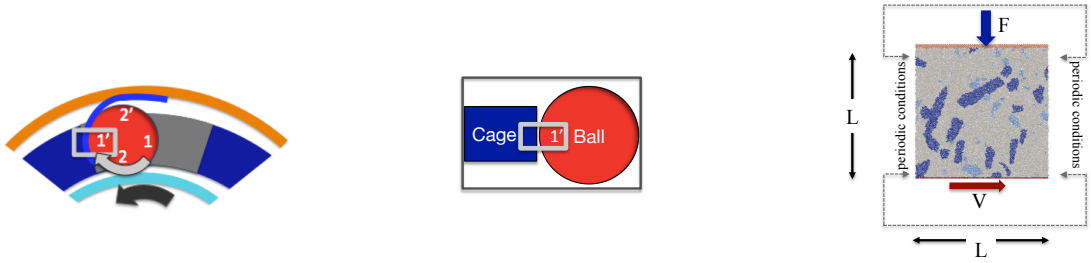

(a) (b) (c)

Figure 1 – (a) Scheme of the double transfer mechanism. The zones 1, 1', 2 and 2' are used as a reference to point the orientation of the ball and the contact ball/cage. A first contact is made between the cage and the ball: see zone 1'; then the ball transfers the transfer film (also known as third body) to the races. (b) Zoom of the contact cage-ball. (c) Scheme of the mechanical boundary conditions applied on a composite (PGM-HT) numerical sample of size L, under tribological conditions, with a force F applied on the top, and a shearing speed v applied in the bottom representative of the speed of the ball.

behaviour of materials [9] (as elastic modulus, density or Poisson's ratio) and the local tribological behaviour (detachment, agglomeration of third body particles). Such laws must be included in a composite geometric model of the proportions and shapes of its components (matrix and / or reinforcements and / or fillers...). Experiment analyses are carried out to inform the model. X-Ray tomography and Atomic Force Microscopy (AFM) analyses are made to identify the volume fraction of the components (fibre, MoS_2 and PTFE) and the adhesion between them, respectively. Constituent data obtained from experimental analyses are shown in *Section 2*. Then, model hypothesis are presented and are related to the experimental results in *Section 3*. Finally, results obtained by DEM simulations are shown in *Section 4*.

2. EXPERIMENTAL CHARACTERISATIONS

In order to create the numerical sample, several information is necessary: 1) the composite composition (from a material and a geometrical point of view), 2) an estimation of the size of the representative element volume and 3) the interaction laws and adhesion values between the different elements of the model. To fulfil the three previous points, three characterisations are realised: 1) observations by Scanning Electron Microscopy (SEM), 2) observations by X-ray tomography and 3) adhesion measurements by atomic force microscopy (AFM). The sample of the self-lubricating material used for observation is cylindrical, and has a length of 12 mm, and a diameter of 7 mm. The material observed was PGM-HT, produced by JPM Mississippi (USA). This sample is the same that the one used in [4] for the tribological testing (same batch, same machining process and it is also preconditioned in vacuum). In order to determine the microstructure and the composition of the composite, two techniques of observations have been used: Scanning Electron Microscopy and X-ray Tomography. With SEM it was possible to have information about the fibres diameter, length, and chemical composition. With X-ray tomography it was possible to build the numerical sample (see section 3.1).

2.1 Microstructure and Composition Studies

For the microstructure analyses SEM observations are carried out. To this end, samples are cut perpendicularly to the axis of the cylinder, at room temperature. Then, the surfaces generated after cutting are observed in a SEM FEI, XL30 (see Fig. 2). It is observed by SEM that fibres of PGM-HT have a diameter of about 20 µm, and their length is of about 100 µm. Regarding MoS_2 particles, their size could reach 100 µm. These results validate the observations made in literature about PGM-HT [3]. It has in fact a coarser microstructure than RT/Duroid 5813 (in which the fibre length can reach 300 µm and their diameter can be smaller than 3 µm, while the MoS_2 particles have a size of about 10 µm). EDX analyses are carried out on the fibres of PGM-HT in order to identify their components. The following elements were found: Si, Al, O, S, and Ca. According to the chemical composition and to SEM observations, it appears that PGM-HT is composed of E-glass fibres.

After these first characterisations, an X-ray Tomograph High resolution (type tomograph RX Solutions EasyTom Nano – with a resolution of 0.7 μ m per pixel) is used in order to build a realistic 3D image of the microstructure of PGM-HT, and to be able later to build a realistic morphological representation of this composite. For the X-ray analyses, samples of $0.5\times0.5\times0.5$ mm^3 are cut at room temperature. 3D volumes are reconstructed (see Fig 3.) through the ImageJ software and its extension Fiji. Under X-ray, the white areas indicate the presence of MoS_2, light grey areas indicate the presence of glass or mineral fibres (according to the composite), and the black areas are related to the PTFE matrix. X-ray tomography not only allows to visualize in the bulk and in 3D, but also to measure the volume fractions of the components. It appears that the PTFE represents two-thirds of the composites, while glass a quarter and MoS_2 a tenth. Moreover thanks to such observations, it is possible to

have an estimation of the size of the numerical sample, also known as the *representative element volume* (REV).

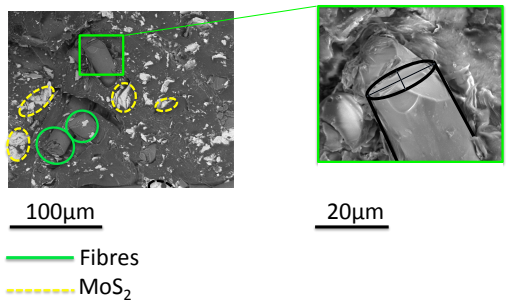

Figure 2 - Internal Structure (sample prepared by rupture at room temperature) of PGM-HT, observed in a SEM with a GSE detector controlled pressure. On the right side: zoom of a fibre.

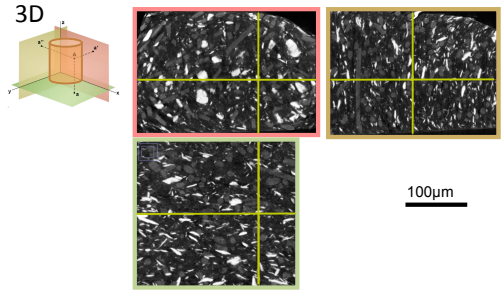

Figure 3 – Images obtained by X-ray tomography of a PGM-HT (white: MoS_2, light grey: fibre, dark grey: PTFE (Matrix)).

The representative element volume (REV) is defined as the volume that should ensure the representative of the whole material. It should contain a high amount of information on the microstructure as the material micro-heterogeneities (fibres, inclusions, etc.), and should be representative of the macroscopic material response [11][12]. The REV size has been selected according to the volume fraction of the heterogeneities (fibres and MoS_2). To do so, 10 REV sizes were tested: from 30 to 380 µm, and the volume fraction of the components is measured. A sample size (or REV size) of 280 µm is chosen because with is it is found a good compromise between the simulation time and the microstructure information.

2.2 Adhesion Interaction Between Composite Components

To identify the adhesive behaviour of the different components of the composite, AFM measures are carried out. In the AFM analysis the adhesion force can be obtained as an output. To perform such measures, a spherical bead of a diameter of 20 µm replaced the sharp tip. This bead was placed on the AFM's cantilever (see Fig. 4). Two bead materials are used: the steel used in ball bearings (AISI 440C) and borosilicate. The latter is
a reference material representative of glass fibres (since E-glass fibres has a high percentage of silica (56%) and it also has bore oxide (~6%)). AFM tests were carried out on the bulk material, and it was ion milled in order to avoid cutting pollution due to PTFE flowing (that can result from cutting with a blade). Once the samples were cut, each component of the composite was identified (PTFE, fibre and MoS_2) by a comparison with its optical view (see Fig. 5). Afterwards, each constituent was put in contact either with the stainless steel AISI 440C bead or with the borosilicate bead.

In Fig. 6 the mean adhesion force for each component of PGM-HT after ion milling is shown. For the AISI 440C bead the pull-off force is higher for PTFE (350±150 nN) and smaller for fibres (85±8 nN). Nevertheless, for the borosilicate bead the pull of force is higher for PTFE (320±180 nN) and smaller for MoS_2 (180±70nN). In both cases, with the exception of PTFE, the components had higher adhesion with the borosilicate bead than with the AISI 440C bead. It is also interesting to note that the error of the PTFE adhesion measurements is considerably higher if it is compared to the other components. This is due to the fact that the PTFE in the composite is not 100% pure, it is the result of the mixture of different components (as stabilizers, flame retardants, etc. This effect can also be a consequence of the fabrication process of the composite, in which debris of MoS_2 and fibres might get mixed with the matrix). Overall, the values of adhesion measured by AFM permit the construction of a representative numerical model from a point of view of the components' interaction. In fact, in the model the laws used to represent each material use the adhesion values between the components as an input. Thanks to the different results obtained in the previous section it is now possible to fulfil the numerical model with relevant information.

3. BACK TO THE DISCRETE ELEMENT MODEL

3.1 Building the geometry of the numerical sample

The numerical geometry was built from X-ray tomography images (see Fig. 7-left). The three components of the composite were identified and represented numerically (see Fig. 7-right).

Table 1. Results obtained for PGM-HT from -ray tomography and from SEM observations.

	PGM-HT				
	Composite Elements	**As seen in X-ray Tomography (Fig. 1)**	**Volume Fraction (%)**	**Size (µm)**	**Chemical Components**
Lubricant	MoS_2	The white phase	10±2	$20<L\leq100$	Mo, S
Fibres	E-glass	The light grey phase	24±3	$60<L\leq150$; $\phi\approx20$µm	Si, Al, O, S, Ca
Matrix	PTFE	The dark grey phase	66±6	-	F, C

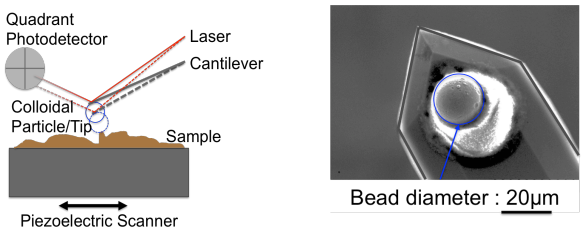

Figure 4 – (Left) AFM Principle. (Right) AFM bead

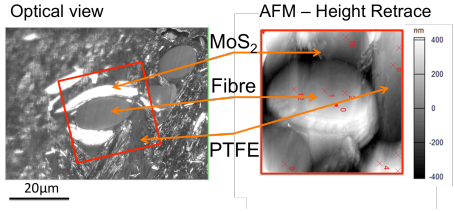

Figure 5 – PGM-HT bulk: Optical view versus AFM view. MoS_2, Fibre and PTFE are identified.

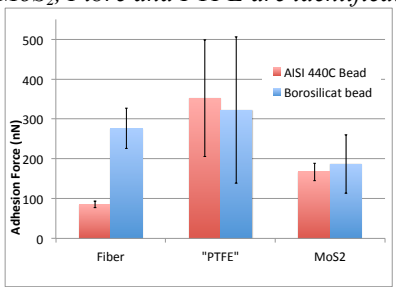

1.1.1 *Figure 6 – AFM mean results of pull-off force for PGM-HT.*

They were identified through the ImageJ software and its extension Fiji, in which a manual threshold tool is used to segment the grey scale images into the features of interest: white (MoS_2), the light grey (fibres), and the black areas (PTFE). Once the components were identified, the images were transformed into numerical images, and discrete particles were deposed. Such discrete particles were assigned in order to identify each component of the sample (see Fig. 6-centre). Once the heterogeneous geometry was created, laws that emulated the material properties were added to the model.

3.2 Emulating materials properties

In the composite material there are three different components (glass fibres, PTFE and MoS_2), and each of then are represented numerically. An interaction law is used to emulate the material properties in the numerical model. For example glass fibres are known as fragile (see Fig. 7–right). Consequently, an interaction law that represents fragile materials is added to the model.

3.2.1 Representing the Behaviour of Glass Fibres

In order to represent glass fibres Cohesive Zone Model (CZM) is used. CZM is a type of interaction law that has been used previously to represent fragile bodies in DEM models. For example, CZM is successfully used to represent fragile carbon/carbon composites, and to study the wear mechanisms of these materials [10]. CZM is based on the following parameters: the decohesion energy w (the surface under the curve of Fig. 8), the normal interaction stiffness C_n, the viscosity associated with the evolution of inter-particle adhesion β. In Fig. 8 an example of a typical CZM graph is shown, in which r^* is the elastic stress limit and δ_c is the distance that defines the elastic range (without damage). The intensity of the inter-particle damage is characterized in this model by β, it takes a value between 0 and 1: 1 if there is no damage, and 0 if the link is totally damaged. For the purposes of this work, the initial interactions are perfectly intact ($\beta = 1$) and the normal and tangential stiffness are considered equal. As a result, the local model is defined by two parameters: C_n and w. [10]

3.2.2 Representing the behaviour of PTFE

PTFE is known as a ductile material (see Fig. 9–a). In order to represent PTFE, a specific law based on two parameters is used (see Fig. 9-b). Such parameters are the distance of attraction X that defines the attraction area of each element, and the attraction intensity force γ, that represents the constant force in opposition to element separation. With the use of long distances of attraction ($x \geq d$, in which d is the discretisation diameter), a network of interaction is generated within the particles [5] and the cooperative movements of the particles are promoted, allowing then to emulate the plasticity of the material. In order to explain the chart of Fig. 9-b, the reacting force between two particles will be as "Force", and the distance between the particles as "distance".

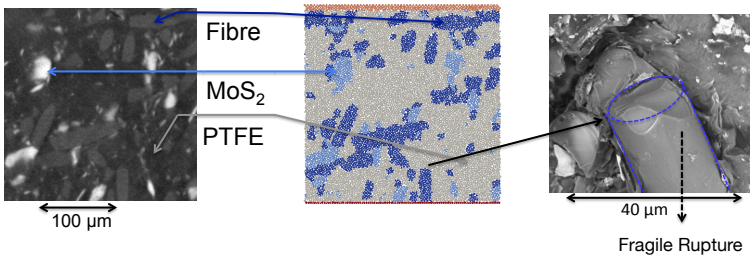

Figure 7 – A X-ray Tomography observation (left) used to build the numerical sample (centre) of PGM-HT. And (right) the fragile rupture of the fibre.

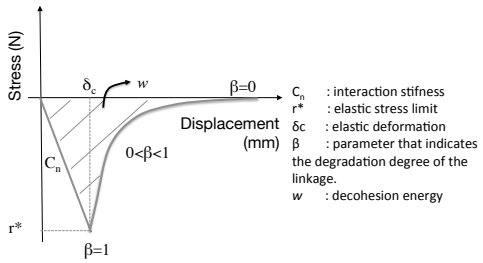

Figure 8 – Cohesive Zone Model (CZM) graph.

If element attraction areas do not overlap, there is no interaction between elements (Force = 0 and distance > *X*), as shown in zone 3 of Fig. 9-b. If element attraction areas do overlap, and the distance between the bodies is not equal to zero (0 < distance < *X*), an attraction force that decreases inversely proportional to the distance between two elements acts on each element, as shown in zone 2 of Fig. 9-b. This force can reach a maximal value of γ. Finally, if the distance between elements is equal to zero, a repulsive force acts on each element to avoid penetration as shown in zone 1 of Fig. 9-b.

To observe the global behaviour of a medium managed by the previous interaction law, a compression test on a circular sample (of a diameter of 0.1 mm) is performed. The sample is compressed until a deformation of 25% is reached, and it is made of a collection of elements of diameter equal to d (see Fig.10)). After testing different parameters (as the cohesion and the elasticity under compression, discretization size, etc.) in order to make the model representative of the behaviour of PTFE, it was found that the cohesion parameter "γ" has a strong influence on the plastic plateau of the curves: when the material cohesion decreases, the plastic *plateau* is found for smaller zones of stress (see Fig.11). With respect to the effect of parameter *"k"*, it is observed that its effect is less marked on the stress-strain curves. Nonetheless, it is still possible to observe at the leftmost part of the curve a certain influence on the slopes of the curves. For instance, the criteria selection for the representativeness of the material will be based on the zone of its plastic *plateau*. A value of γ = 0.4 N is selected because the plastic plateau obtained is in the same order of magnitude that the plastic *plateau* obtained for PTFE in experimental tests [13]. A discretization size of 3e-3 mm is selected because with it is obtained a good compromise between the material representation and the simulation time.

3.2.3 Representing the behaviour of the MoS_2

Tedstone et al were able to build the stress-stress curves for MoS_2 [14]. They observed a plastic behaviour in the stress-strain curve of MoS_2 and calculated the compressive stress required to obtain plastic deformation in MoS_2. For the purpose of this work, the behaviour of MoS_2 is represented at a microscopic scale. A compression test on a circular sample is also performed in order to observe the global behaviour of a medium managed by the previous interaction law. The sample of MoS_2 has the same dimensions than for the case of PTFE, and it is also compressed until a deformation of 25% is reached. After testing different distances of interaction "*X*": *X*=2d, *X*=d, *X*=d/10, and *X*=d/20 (in which d is the discretization diameter) a value of *X*=d/10 was selected because it is thought to be a good compromise to represent both the plasticity of MoS_2 and its interlayer sliding behaviour (that creates a sort of fragile failure). For MoS_2, higher cohesion values were tested: 125 γ < γ <20 (as for PTFE, γ =4e-1 N). It was found that cohesion values of 150 γ was accurate to represent the plastic plateau of MoS_2 as reported in [14].

4. TRIBOLOGICAL SOLLICITATIONS

4.1 Model description

Once the geometry of the sample was created and that the material properties were emulated. (as shown in section 3.1.1 and 3.1.2 respectively), tribological test were performed. The simulated system is two-dimensional (see Fig. 7, and see simulation parameters in Tab. 2). The sample for tribological tests is informed with the values of interaction between the components measured by AFM shown in Fig. 6. To do so, the mean values of adhesion resulting from AFM analyses were used as an input. Additionally, different properties were studied numerically as complement to the experimental measurements. For example, the effect of having three different kinds of matrices: a matrix with a lower cohesion (γ */10)*, a "reference" cohesion (γ *)*, and another with a higher cohesion (10γ). The sample is composed of 9000 rigid particles (this number of

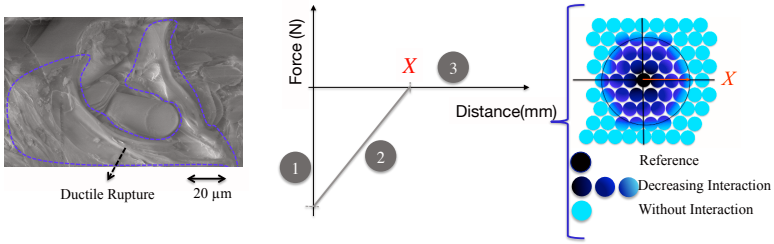

(a) (b) (c)

Figure 9 – (a) Representative chart of the Interaction law used. (b) Interaction of the particules at a distance X = d.

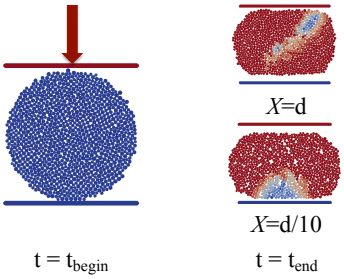

Figure 10 – Example of the configuration of compression tests for two distances "x". x = d and x = d/10. For the latter case a sort of brittle behaviour is induced.

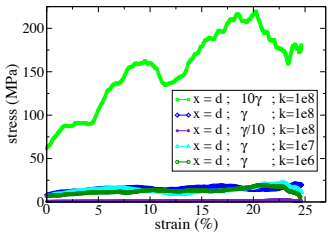

Figure 11 – Engineering Stress-strain under compression. Stress is calculated according to Eq.1 .Curves for the different parameters tested to represent PTFE.

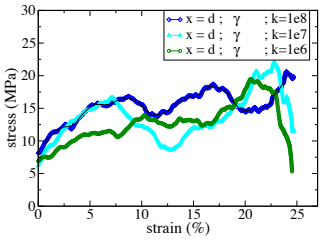

Figure 12 – Stress-strain curves for PTFE samples. Influence of

particles is considered to give a good compromise between the material representation and the simulation time). A polydispersity of 20% is considered in order to prevent crystallization effect in the discretization [15]. The material is sheared between two parallel rough walls, of length L, distant from L. Periodic boundary conditions are applied along the shear direction (lateral boundaries): No particles get out of the contact (wear flow is equal to zero). The wall's roughness is made with a set of grains with the same size polydispersity than the sample discretization. The upper wall, summited to a pressure P (see values in Table 2), is connected to the packing with the same interaction law that the PTFE matrix (see section 3.1.2.2). The lower wall moves with a constant speed V, interacts with the packing according to the unilateral cohesive law, with Coulomb friction. The material used for this wall is AISI 440C.

Table 2 - Simulation parameters (nominal values) for tribological solicitations.

Average particle diameter (d)	3e-3 mm
Polydispersity (on diameter)	20%
Sample Height and Length (L)	0.3 mm
Pressure (P)	50 MPa
Speed (V)	2 mm/ms
Time step (dt)	2e-6s
Simulation time (t)	0.16s
γ	4e-1N

4.2 Results

4.2.1 Stress Profile

In discrete media, the notion of internal moments is used for the calculation of the stress tensor. These tensors are calculated for the volume of the sample, v. They are named σ_{ij} and are estimated between two particles i and j, and for a contact α, as follows [16]:

$$\sigma_{ij} = \frac{1}{v} \sum_{\alpha=1}^{N_c} l_i^{\alpha} \otimes r_j^{\alpha} \qquad (1)$$

In which l is the inter-centre vector between the particles, r is the reaction force at the contact, and N_c is the total number of contacts. It is possible to calculate these tensors for different areas of the media. In Fig. 13 (a) the distribution of the component σ_{12} of the stress tensor for P = 50MPa for the matrices tested is shown. When the cohesion of the matrix is higher, it resists more to shear. This resistance creates an action-reaction effect within each layer, which resists to their deformations and increases the deviations in the stress profiles. So, these deviations are related to the resistance of the material to shear. In Fig. 13 (a) it is possible to observe the images of the simulation for the three types of matrices tested. It is possible to observe that the matrix with the lower cohesion (matrix0) is almost completely sheared along the sample height. Instead, if the cohesion of the matrix increases, the material is subjected to higher stresses that may lead to a higher internal damage, and to a higher presence of fibres in the 3rd body. In order to study the effect of changing the cohesion of the other components and to compare them with those obtained for the matrix, the cohesion of MoS_2 was changed, as well as the interaction between the matrix and MoS_2. The lower values of cohesion correspond to the subscript "0" and the higher values correspond to the subscript "2". It can be seen that varying the cohesion of MoS_2 and the interaction between matrix-MoS_2 has a smaller effect than the matrix in the stress that is inside the material Fig. 13 (b). These results confirm the theory of composite materials in which the primary role of the matrix is "to act as a medium for transferring the load to the components", apart of holding the components together [17].

4.2.2 Internal Damage in the composite

In order to study the internal damage inside the composite, the evolution of the interactions between the matrix and fillers are studied. In Fig. 14 it is possible to observe the evolution of the interactions matrix-MoS_2 and matrix-fibre. It is observed that when the matrix cohesion increased, the interactions between the matrix and the components of the composite were smaller than for the low cohesion matrix. As it was mentioned previously, when the cohesion of the matrix is higher the material resists more to be sheared, and the stress

inside the material increases and the damage is promoted. This leads to a reduction of the interaction between the matrix and the fillers.

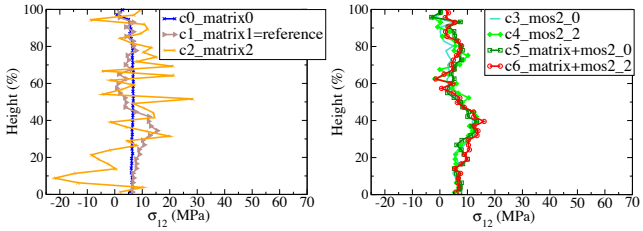

(a) (b)

Figure 13 –Distribution of the component σ_{12} of the stress tensor for: (a) a matrix with low cohesion c0_matrix0, another with an intermediate cohesion c1_matrix1, and an highly cohesive matrix: c2_matrix2, and (b) for the rest of the components.

4.2.3 Third body

The cohesion of the matrix has also an influence on the third body composition. A low cohesive matrix is completely sheared and the third body is of the length of almost all the sample size. If the material is completely sheared, this it is not interesting for applications as a cage material because a non stable third body layer is formed. What it is interesting is a material capable to generate a stable third body, and to provide a good lubrication while it is degraded. When an intermediate matrix cohesion is used, the third body is found to be a mixture of MoS_2, PTFE, and small particles of fibre (see matrix1). This type of third body composition has also been observed in experimental work carried out by [4]: « the third body is a material composed of a mix of PTFE, MoS_2 and fragmented glass fibres ». When the matrix cohesion increases, the presence of bigger particles of fibre and MoS_2 in the third body is promoted. This is due to the fact that when the matrix cohesion is higher, the interactions between the matrix and the fillers are more susceptible to damage. This will promote detachment of big particles of the fillers (MoS_2 and Fibres) from the matrix to the third body. In Fig. 15 images at the end of the simulation for the three types of matrix are shown. It is possible to observe that for the matrix with the highest cohesion value (matrix 2), a big fibre particle is present in the third body layer.

This was not observed for the matrices with smaller cohesion. The evolution of the interactions between the matrix and the metal surface are studied. In Fig. 15 it is observed that when matrix cohesion is low (matrix 0), the interactions matrix-metal remain with almost no variation. This is because the whole material is being sheared. When the matrix cohesion increases, the number of interactions between the matrix and the the metal decreases. This is due to the fact that the material is being degraded : the fillers come out of the bulk material and start also to interact with the metal surface, so the third body is a mixture of matrix and fillers.

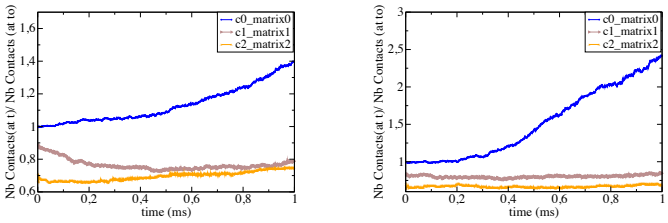

(a) **(b)**

Figure 14 – Evolution of the interactions (a) matrix-fibre and (b) matrix-mos2 for Matrix 0 (lower cohesion value), Matrix 1 and matrix 2 (higher cohesion value).

5. CONCLUSIONS AND LESSONS LEARNED

This work is focused on the study of self-lubricating materials by coupling experimental analyses with numerical modelling. With the experimental analyses information about the material is obtained. Such information is used to inform the model with realistic data (as the material geometry, volume fraction, interaction between the components, etc.) With the numerical tests, the objective is to be able to have a predictability of the behaviour self-lubricating materials in order to understand the lubrication mechanisms of self-lubricating materials (as the connection between the experimental and the numerical samples can be effectively made in terms of the proportions and shapes of its components). Since in previous work the importance of the composite microstructure (and fibre length) on the tribological performances of self-lubricating materials is pointed out [3][4], with this technique it is possible to study the role and impact of

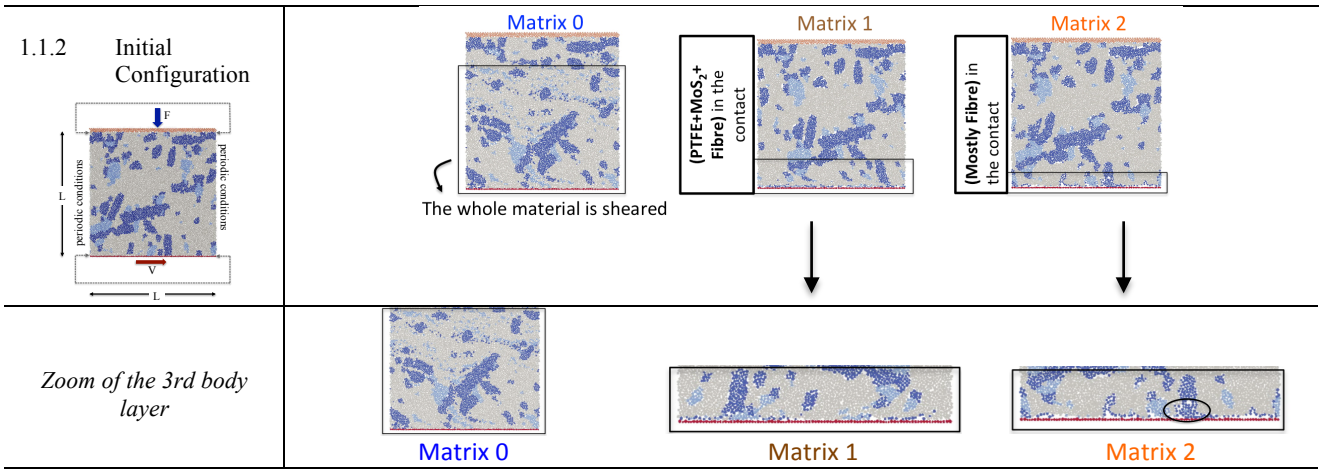

Figure 15 – Images at the end of the simulation time for the three matrices rested. Matrix 0 with the lower cohesion, matrix 1 with an "intermediate" cohesion, and matrix 2 with the higher cohesion.

the different constituents and microstructures.

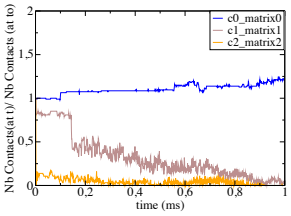

Figure 15 – Evolution of the interactions (a) matrix-metal for Matrix 0 (lower cohesion value), Matrix 1 and matrix 2 (higher cohesion value).

For example, in previous DEM studies with self-lubricating materials [5] it has been observed that the fibre length and the microstructure does have an effect on the third body composition, particularly on the presence of fibres in the third body. With these studies it is also possible to verify that the matrix has an important role in the load transfer and also in the third body composition. Moreover, it is possible to reproduce some behaviours observed experimentally, as the presence of a mix of PTFE, MoS_2 and fragmented glass fibres in the third body composition. From a numerical point of view, it is possible to calibrate the numerical parameters in order to ensure an appropriate representativeness of the materials. This is achievable by carrying out numerical tests (as traction, compression, shearing tests, etc.), and by comparing the results with those obtained experimentally. Further studies of DEM are on-going and they are targeted to represent the double transfer of such self-lubricating materials. Such studies will be able to provide further information about the influences of parameters as the microstructure and the matrix cohesion in the generation and quality of the double transfer layer. Similarly, it is envisaged study in those tests the effect of having different atmospheres (as vacuum, air). This is possible by informing the model with adhesion values between the components resulting from different atmospheres.

4. ACKNOLEDGEMENTS

The authors would like to thank CNES and SKF for supporting the study. The authors would also like to thank the Material Science Laboratory of the INSA Lyon: MATEIS, particularly to J. Adrien for his support in the X-ray tomography measurements.

5. REFERENCES

[1] "NASA's Jupiter-circling Spacecraft Stuck Making Long Laps," *US News & World Report*. [Online]. Available: https://www.usnews.com/news/news/articles/2017-02-23/nasas-jupiter-circling-spacecraft-stuck-making-long-laps. [Accessed: 20-Jun-2017].

[2] EW Roberts, "Space tribology: its role in spacecraft mechanisms," *IOP Publ.*, 2012.

[3] J. Sicre, Y. Michel, E. Videira, L. Nicollet, and D. Baud, "PGM-HT as DUROID 5813 Replacement ? Lifetime Results on STD Scanning Earth Sensor and Polder Bearing Shaft," ESMATS, Vienna, Austria, p. 8, Sep-2009.

[4] G. Colas, A. Saulot, S. Descartes, Y. Michel, Y. Berthier, "Double Transfer Experiments to Highlight Design Criterion for future Self-lubricating Materials," ESMATS, Bilbao, Spain, p. 8, Sep-2015.

[5] M.D. Villavicencio Rojas, et al., "Self-lubricating composite bearings: Effect of fibre length on its tribological properties by DEM modelling," *Tribology International*, 2016.

[6] Josephine Cunningham, Robert A Rowntree, "RT/Duroid 5813 Replacement Investigation." [Online]. Available: http://articles.adsabs.harvard.edu/cgi-bin/nph-iarticle_query?bibcode=1997ESASP.410...97C&db_key=AST&page_ind=0&data_type=GIF&type=SCREEN_VIEW&classic=YES. [Accessed: 07-May-2017].

[7] A. Merstallinger, C. Macho, G. Brodowski-Hanemann, H.Bieringer, "SLPMC - New Self Lubricating Polymer Matrix Composites for Journal and Ball Bearing Applications in Space," ESMATS, Bilbao, Spain, p. 8, Sep-2015.

[8] C. Macho, A. Merstallinger, G. Brodowski-Hanemann, M. Palladino, L. Pambaguian, "SLPMC - Self Lubricating Polymer Matrix Composites," ESMATS, The Netherlands, 2013.

[9] M. Renouf, H. -P. Cao, V. -H. Nhu, "Multiphysical modeling of third-body rheology," *Tribol Int*, vol. 44, pp. 417–425, 2011.

[10] M. Champagne, M. Renouf, Y. Berthier, "Modeling Wear for Heterogeneous Bi-Phasic Materials Using Discrete Elements Approach," vol. 136, no. 21603, pp. 1–11, 2014.

[11] C. Pelissou et. al, "Determination of the size of the representative volume element for random quasi-brittle composites," *International Journal of Solids and Structures*, pp. 2842–2855, 2009.

[12] A. Zaoui, "Changement d'échelle: motivation et méthodologie," in *Homogénéisation en mécanique des matériaux, Tome 1 : Matériaux aléatoires élastiques et milieux périodiques*, P. Bornert M. ..Bretheau, T. ..Gilormini, Ed. Hermes science, 2001, pp. 19–39.

[13] Du Pont, *Teflon PTFE . Properties Handbook*. USA.

[14] A. A. Tedstone *et al.*, "Mechanical Properties of Molybdenum Disulfide and the Effect of Doping: An in Situ TEM Study," *ACS Appl. Mater. Interfaces*, vol. 7, no. 37, pp. 20829–20834, Sep. 2015.

[15] Lätzel, M., Luding, S., Herrmann, H.J., "From discontinous models towards a continuum description. In : Vermeer, P.A., Diebels, S.Ehlers, W., Herrmann, H.J., Luding, S., Ramm, E. (eds). Continous and Discontinous Modelling of Cohesive-Frictional Materials.," in *Lecture Notes in Physics*, 2001, vol. 568, p. 215.

[16] F. Radjaï, F. Dubois, *Discrete Modeling of Granular Materials*. Wiley, 2011.

[17] S. Rana and R. Fangueiro, *Fibrous and Textile Materials for Composite Applications*. Springer, 2016.